

Orthonitridoborate Ions $[\text{BN}_3]^{6-}$ in Oxonitridosilicate Cages: Synthesis, Crystal Structure, and Magnetic Properties of $\text{Ba}_4\text{Pr}_7[\text{Si}_{12}\text{N}_{23}\text{O}][\text{BN}_3]$, $\text{Ba}_4\text{Nd}_7[\text{Si}_{12}\text{N}_{23}\text{O}][\text{BN}_3]$, and $\text{Ba}_4\text{Sm}_7[\text{Si}_{12}\text{N}_{23}\text{O}][\text{BN}_3]$

Michael Orth, Rolf-Dieter Hoffmann, Rainer Pöttgen, and Wolfgang Schnick*^[a]

Abstract: The isotopic title compounds $\text{Ba}_4\text{Pr}_7[\text{Si}_{12}\text{N}_{23}\text{O}][\text{BN}_3]$, $\text{Ba}_4\text{Nd}_7[\text{Si}_{12}\text{N}_{23}\text{O}][\text{BN}_3]$, and $\text{Ba}_4\text{Sm}_7[\text{Si}_{12}\text{N}_{23}\text{O}][\text{BN}_3]$ were prepared by reaction of Pr, Nd, or Sm, with barium, BaCO_3 , $\text{Si}(\text{NH})_2$, and poly-(boron amide imide) in nitrogen atmosphere in tungsten crucibles using a radiofrequency furnace at temperatures up to 1650°C . They were obtained as main products ($\approx 70\%$) embedded in a very hard glass matrix in the form of intense dark green (Pr), orange-brown (Sm), or dark red (Nd) large single crystals, respectively. The stoichiometric composition of $\text{Ba}_4\text{Sm}_7[\text{Si}_{12}\text{N}_{23}\text{O}][\text{BN}_3]$ was verified by a quantitative elemental analysis. According to the single-crystal X-ray structure determinations (Ba_4 -

$\text{Ln}_7[\text{Si}_{12}\text{N}_{23}\text{O}][\text{BN}_3]$, $Z=1$, $P\bar{6}$ with $\text{Ln}=\text{Pr}$: $a=1225.7(1)$, $c=544.83(9)$ pm, $R1=0.013$, $wR2=0.030$; $\text{Ln}=\text{Nd}$: $a=1222.6(1)$, $c=544.6(1)$ pm, $R1=0.017$, $wR2=0.039$; $\text{Ln}=\text{Sm}$: $a=1215.97(5)$, $c=542.80(5)$ pm, $R1=0.047$, $wR2=0.099$) all three compounds are built up by a framework structure $[\text{Si}_{12}\text{N}_{23}\text{O}]^{23-}$ of corner-sharing SiX_4 tetrahedrons ($\text{X}=\text{O}, \text{N}$). The oxygen atoms are randomly distributed over the X positions. The trigonal-planar orthonitridoborate ions $[\text{BN}_3]^{6-}$ and also the $\text{Ln}(3)^{3+}$

are situated in hexagonal cages of the framework (bond lengths $\text{Si}-(\text{N}/\text{O})$ 169–179 pm for $\text{Ln}=\text{Pr}$). The remaining Ba^{2+} and Ln^{3+} ions are positioned in channels of the large-pored network. The trigonal-planar $[\text{BN}_3]^{6-}$ ions have a B–N distance of 147.1(6) pm (for $\text{Ln}=\text{Pr}$). Temperature-dependent susceptibility measurements for $\text{Ba}_4\text{Nd}_7[\text{Si}_{12}\text{N}_{23}\text{O}][\text{BN}_3]$ revealed Curie–Weiss behavior above 60 K with an experimental magnetic moment of $\mu_{\text{exp}}=3.36(5) \mu_{\text{B}}/\text{Nd}$. The deviation from Curie–Weiss behavior below 60 K may be attributed to crystal field splitting of the $J=9/2$ ground state of the Nd^{3+} ions. No magnetic ordering is evident down to 4.2 K.

Keywords: boron • oxonitrides • magnetic properties • solid-state structures • silicon

Introduction

Owing to their very high stability both binary boron nitride (BN) and silicon nitride (Si_3N_4) have gained increasing relevance for the development of ceramic materials with manifold applications.^[1] Since both binary compounds have high melting points and show very low interdiffusion coefficients, the synthesis of ternary and higher silicon boron nitrides seems to be difficult by a direct reaction of BN and Si_3N_4 . Recently, X-ray amorphous $\text{Si}_3\text{B}_3\text{N}_7$ has been obtained by Jansen et al. by pyrolysis of the molecular single-source precursor trichlorosilylamino-dichloroborane (TADB; $\text{Cl}_3\text{SiNHBCl}_2$).^[2]

Structural models have been developed for this compound, which are in accordance with the spectroscopic data. A highly cross-linked network of corner-sharing trigonal-planar BN_3 groups and SiN_4 tetrahedrons seems reasonable. All of the nitrogen atoms should be covalently bound to three B and/or Si atoms, respectively.^[3] Thus, both boron and silicon exhibit analogous coordination numbers as in their binary nitrides h -BN, α -, and β - Si_3N_4 , respectively.^[1]

Recently, we have established a straight-forward synthetic approach leading to alkaline earth and rare-earth nitridosilicates by the reaction of silicon diimide $\text{Si}(\text{NH})_2$ with the respective metals in a radiofrequency (rf) furnace.^[4] X-ray amorphous but reactive silicon diimide was obtained by the ammonolysis of SiCl_4 followed by the pyrolysis in a stream of gaseous ammonia at temperatures between 300 – 600°C . An analogous reaction starting from BBr_3 yields a B/N/H polymer. The reaction of this X-ray amorphous poly(boron amide imide) together with metals results in the formation of crystalline nitridoborates.^[5]

Targeting oligonary silicon boron nitrides we have started to investigate the reaction of both silicon diimide and

[a] Prof. Dr. W. Schnick, Dipl.-Chem. M. Orth, Dr. R.-D. Hoffmann, Prof. Dr. R. Pöttgen
Department of Chemistry
University of Munich (LMU)
Butenandtstrasse 5 - 13 (block D)
81377 Munich (Germany)
Fax: (+49) 89-2180-7440
E-mail: wsc@cup.uni-muenchen.de

poly(boron amide imide) with metals by utilizing radiofrequency furnaces. During these investigations we have obtained three new isotopic compounds as coarsely crystalline products with the initially postulated formula $\text{Ba}_3\text{Ln}_8\text{[Si}_{12}\text{N}_{24}\text{][BN}_3\text{]}$ with $\text{Ln} = \text{Pr}, \text{Nd}, \text{and Sm}$. Subsequently a more detailed investigation by single-crystal X-ray crystallography, magnetic measurements, and quantitative elemental analysis revealed these products to be oxonitrides with the formula $\text{Ba}_4\text{Ln}_7\text{[Si}_{12}\text{N}_{23}\text{O][BN}_3\text{]}$. Apparently, the rare earth metals employed were contaminated to a small extent with the respective oxide, and thus oxygen was incorporated into the products. To improve the yield we then introduced BaCO_3 as an additional starting material.

Results and Discussion

The single-crystal X-ray diffraction analysis revealed trigonal-planar (D_{3h}) orthonitridoborate ions $[\text{BN}_3]^{6-}$ (Figure 1), which are situated in the hexagonal cages of a $[\text{Si}_2\text{X}_{24}]$ ($\text{X} = \text{N}, \text{O}$) framework structure, which is built up of corner-sharing SiX_4 tetrahedrons (Figure 2). Despite being isosteric, this $[\text{Si}_{12}\text{N}_{23}\text{O}]$ framework structure exhibits no analogy to the Si-N

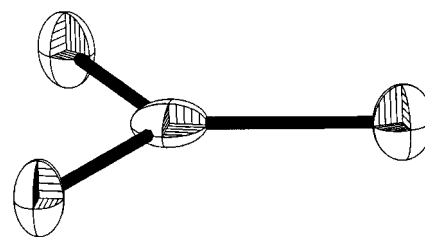


Figure 1. The trinitridoborate ions in $\text{Ba}_4\text{Pr}_7\text{[Si}_{12}\text{N}_{23}\text{O][BN}_3\text{]}$ exhibit point symmetry D_{3h} (ORTEP plot, thermal ellipsoids with 70% probability, B-N distance 147.1(6) pm).

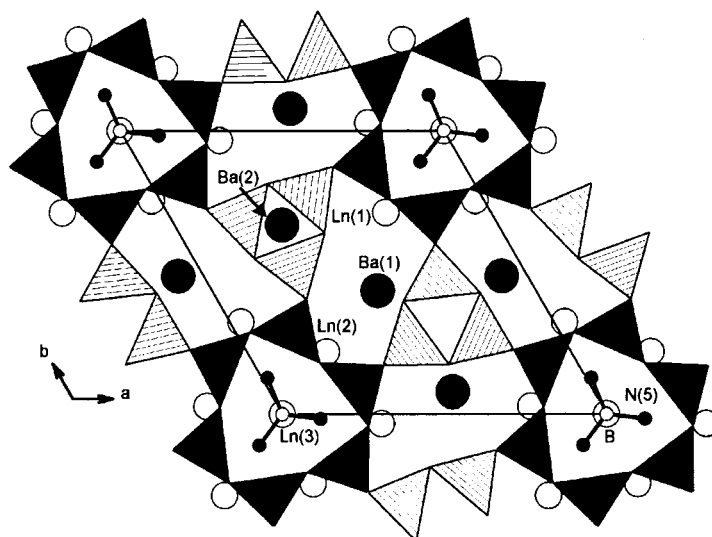


Figure 2. Projection of the $\text{Ba}_4\text{Pr}_7\text{[Si}_{12}\text{N}_{23}\text{O][BN}_3\text{]}$ structure along $[001]$. The $\text{Si}(\text{N/O})_4$ tetrahedrons are depicted as closed polyhedrons.

Abstract in German: Die Umsetzung der Lanthanoide Pr, Nd bzw. Sm mit Barium-Metall, BaCO_3 , $\text{Si}(\text{NH})_2$ sowie Poly(boramidimid) in Tiegeln aus Wolfram bei Temperaturen bis 1650°C im Hochfrequenzofen unter Stickstoff-Atmosphäre führte zur Synthese der drei isotypen Verbindungen $\text{Ba}_4\text{Ln}_7\text{[Si}_{12}\text{N}_{23}\text{O][BN}_3\text{]}$ mit $\text{Ln} = \text{Pr}, \text{Nd}$ bzw. Sm. Die Verbindungen wurden als Hauptprodukte ($\approx 70\%$) eingebettet in außerordentlich harten glasartigen Phasen in Form großer dunkelgrüner (Pr), orange-brauner (Sm) bzw. dunkelroter (Nd) Einkristalle erhalten. Die Zusammensetzung von $\text{Ba}_4\text{Sm}_7\text{[Si}_{12}\text{N}_{23}\text{O][BN}_3\text{]}$ wurde durch quantitative Elementaranalyse bestätigt. Nach Einkristall-Röntgenstrukturanalysen ($\text{Ba}_4\text{Ln}_7\text{[Si}_{12}\text{N}_{23}\text{O][BN}_3\text{]}$, $Z=1$, $P6\bar{3}$ mit $\text{Ln} = \text{Pr}$: $a=1225.7(1)$, $c=544.83(9)$ pm, $R1=0.013$, $wR2=0.030$; $\text{Ln} = \text{Nd}$: $a=1222.6(1)$, $c=544.6(1)$ pm, $R1=0.017$, $wR2=0.039$; $\text{Ln} = \text{Sm}$: $a=1215.97(5)$, $c=542.80(5)$ pm, $R1=0.047$, $wR2=0.099$) liegt in allen drei Verbindungen eine Raumnetzstruktur eckenverknüpfter SiX_4 -Tetraeder $[\text{Si}_{12}\text{N}_{23}\text{O}]^{23-}$ vor ($\text{X} = \text{O}, \text{N}$), in der die Sauerstoffatome statistisch auf die X-Positionen verteilt sind. Die trigonal planaren Orthonitridoborat-Ionen $[\text{BN}_3]^{6-}$ sowie die $\text{Ln}(3)^{3+}$ sind in hexagonalen Käfigen dieses Gerüsts eingelagert (Bindungslängen $\text{Si}-(\text{N/O})$ 169–179 pm, für $\text{Ln} = \text{Pr}$). Die verbleibenden Ba^{2+} - sowie Ln^{3+} -Ionen finden sich in den restlichen Kanälen der Gerüststruktur. Die trigonal planaren $[\text{BN}_3]^{6-}$ -Ionen haben B-N-Bindungslängen von 147.1(6) pm (Wert für $\text{Ln} = \text{Pr}$). Temperaturabhängige Suszeptibilitätsmessungen an $\text{Ba}_4\text{Nd}_7\text{[Si}_{12}\text{N}_{23}\text{O][BN}_3\text{]}$ ergaben Curie-Weiss-Verhalten oberhalb von 60 K mit einem experimentell bestimmten magnetischen Moment von $\mu_{\text{exp}} = 3.36(5) \mu_B/\text{Nd}$. Die Abweichung vom Curie-Weiss-Verhalten unterhalb von 60 K wird auf Kristallfeld-Aufspaltungen des $J=9/2$ Grundzustands der Nd^{3+} -Ionen zurückgeführt. Bis 4.2 K konnte keine magnetische Ordnung nachgewiesen werden.

substructure in Li_2SiN_2 . This lithium nitridosilicate likewise is built up of corner-sharing SiN_4 tetrahedrons.^[6] Also in Li_2SiN_2 all N atoms (N^{2-}) are bound to two neighboring Si atoms and the respective bond lengths are similar (Si-N^{2-} 169–179 pm; Li_2SiN_2 : 173–181 pm).^[6] However the angles $\text{Si-N}^{2-}\text{-Si}$ in $\text{Ba}_4\text{Pr}_7\text{[Si}_{12}\text{N}_{23}\text{O][BN}_3\text{]}$ vary in a significantly larger range ($123\text{--}173^\circ$) as compared with Li_2SiN_2 ($108\text{--}121^\circ$),^[6] though the values are still in an acceptable range for nitridosilicates. The most enlarged angle ($\text{Si-N}(\text{O})(2)\text{-Si}$ 173°) is found at the edges of the hexagonal Si-N cage surrounding the $[\text{BN}_3]^{6-}$ ions (Figure 3). However a localization of solely oxygen on this site seems unreasonable.

Prior to this work only two compounds have been identified that contain orthonitridoborate ions $[\text{BN}_3]^{6-}$, namely $\text{Ce}_{15}\text{B}_8\text{N}_{25}$ ^[7] and $\text{La}_5\text{B}_4\text{N}_9$.^[8] In accord with the formulation $(\text{Ce}^{4+})_6(\text{Ce}^{3+})_9[\text{BN}_3^{6-}]_8\text{N}^{3-}$ the mixed-valence cerium compound is supposed to contain $[\text{BN}_3]^{6-}$ units and “isolated” nitride ions as well. In $(\text{La}^{3+})_5[\text{BN}_3]^{6-}[\text{B}_3\text{N}_6]^{9-}$ monomeric orthonitridoborate ions and cyclotritritridoborate species have been found. The latter ones also have been identified in nitridoborates like $\text{Pr}_3\text{B}_3\text{N}_6$.^[5] Bond lengths and angles (B-N 147.1(6) pm; N-B-N 120°) of the orthonitridoborate ions in $\text{Ba}_4\text{Pr}_7\text{[Si}_{12}\text{N}_{23}\text{O][BN}_3\text{]}$ correspond well with the values found in $\text{La}_5\text{B}_4\text{N}_9$ (147(2) and 150(2) pm; $118\text{--}123^\circ$),^[8] and $\text{Ce}_{15}\text{B}_8\text{N}_{25}$ (144(4)–149(4) pm and $114(1)\text{--}127(1)^\circ$)^[7] and they are similar to those in hexagonal boron nitride (145 pm, 120°).^[1]

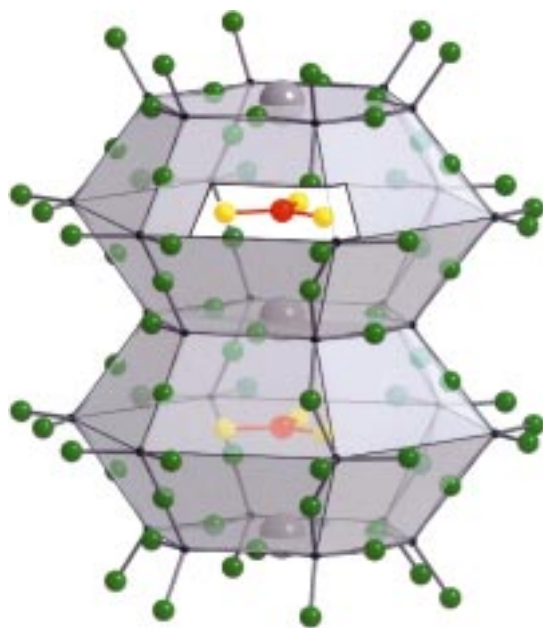


Figure 3. Eighteen corner-sharing $\text{Si}(\text{N}/\text{O})_4$ tetrahedrons form large-pored hexagonal cages built up of $\text{Si}_6(\text{N}/\text{O})_6$ rings. The trinitridoborate ions $[\text{BN}_3]^{6-}$ and the Ln^{3+} ions are located within these cages. The boron, silicon, nitrogen/oxygen, and praseodymium atoms are drawn in red, black, green/yellow, and gray, respectively.

From a topological point of view the $[\text{Si}_{12}\text{X}_{24}]$ framework structure in $\text{Ba}_4\text{Ln}_7[\text{Si}_{12}\text{N}_{23}\text{O}][\text{BN}_3]$ may easily be classified by using the specific distribution of the occurring Si_nX_n ring sizes. The cycle-class sequence^[9] of $\text{Ba}_4\text{Ln}_7[\text{Si}_{12}\text{N}_{23}\text{O}][\text{BN}_3]$, which gives the frequency distribution of the different Si_nX_n ring sizes (with $n = 1, 2, 3, \dots$), amounts to $\{-, 0, 2, 0, 0, 13, 12, 30, 36, 138, 216, 582, \dots\}$. Accordingly, the $[\text{Si}_{12}\text{X}_{24}]$ framework structure of $\text{Ba}_4\text{Ln}_7[\text{Si}_{12}\text{N}_{23}\text{O}][\text{BN}_3]$ contains only corner-sharing SiX_4 tetrahedrons, and all possible ring sizes Si_nX_n except those with $n = 2, 4$, or 5 . Thus, topologically the $[\text{Si}_{12}\text{X}_{24}]$ framework structure of $\text{Ba}_4\text{Ln}_7[\text{Si}_{12}\text{N}_{23}\text{O}][\text{BN}_3]$ significantly differs from the Si–N substructure of Li_2SiN_2 or from formally isosteric network structures of the polymorphic SiO_2 modifications.

The $[\text{Si}_{12}\text{X}_{24}]$ framework structure in $\text{Ba}_4\text{Pr}_7[\text{Si}_{12}\text{N}_{23}\text{O}][\text{BN}_3]$ is suggestive of zeolite or clathrate structures (Figure 4). However, topologically there is no similarity to known aluminosilicate frameworks.^[10] A raw measure for the microporosity of framework structures is given by the framework density (FD). It is defined as the number of tetrahedral centers (T) per 1000 \AA^3 .^[10] Amongst all nitridosilicates with Si–N framework structures known so far, $\text{Ba}_4\text{Pr}_7[\text{Si}_{12}\text{N}_{23}\text{O}][\text{BN}_3]$ exhibits the lowest value of the framework density $\text{FD} = 16.97 \text{ T per } 1000 \text{ \AA}^3$. Accordingly $\text{Ba}_4\text{Pr}_7[\text{Si}_{12}\text{N}_{23}\text{O}][\text{BN}_3]$ is even similar to typical microporous zeolites (FD values for some zeolites in T per 1000 \AA^3 : 17.5 (AlPO₄-5), 17.9 (ZSM-5), 19.3 (Nonasil)).^[10] However due to the differing ionic radii of O^{2-} and N^{3-} a quantitative comparison seems difficult.

The crystal structure of $\text{Ba}_4\text{Pr}_7[\text{Si}_{12}\text{N}_{23}\text{O}][\text{BN}_3]$ contains characteristic 6-ring (6R) ‘channels’ formed by corner-sharing hexagonal cages running along $[001]$ (Figure 2 and Figure 4). Along the c axis $\text{Ln}(3)^{3+}$ ions in the centers of the $\text{Si}_6(\text{N}/\text{O})_6$

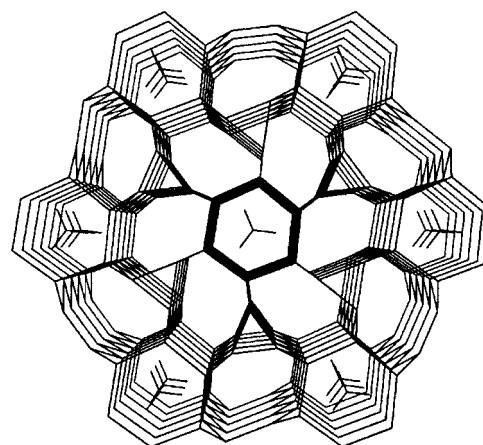


Figure 4. Topology of the framework in $\text{Ba}_4\text{Ln}_7[\text{Si}_{12}\text{N}_{23}\text{O}][\text{BN}_3]$ as a view parallel to $[001]$. For clarity only the centers of the tetrahedrons are connected.

rings and $[\text{BN}_3]^{6-}$ in the centers of the hexagonal cages alternate. The $\text{Ba}(2)^{2+}$ ions are situated in the center of the smaller Si_3X_3 rings. In the centers of the large Si_8X_8 rings there are $\text{Ba}(1)^{2+}$, $\text{Ln}(1)^{3+}$, and $\text{Ln}(2)^{3+}$ ions. The cations are coordinated by the X atoms of the $[\text{Si}_{12}\text{X}_{24}]$ framework structure. The Ba^{2+} ions show a typical coordination environment in which they are in contact with 10 (Ba(1)) or 12 (Ba(2)) anions N/O within distances of 291–355 pm and 318–322 pm, respectively. The atoms Pr(1) and Pr(2) exhibit usual coordination spheres as well. They are coordinated by eight nitrogen atoms within a range from 232–293 pm. The Pr(3)³⁺ ions exhibit a 3+6+3 coordination (Pr(3)–N/O: 245–322 pm) (Figure 5). The observed distances approximately correspond with the respective sums of the ionic radii.^[11, 12]

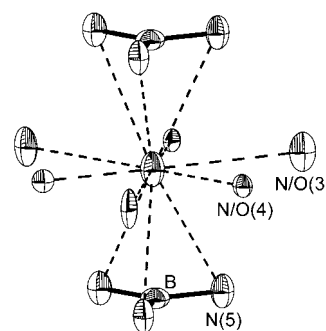


Figure 5. Local environment of the $\text{Ln}(3)$ atoms (anisotropic displacement ellipsoids with 90% probability) shows a coordination of 3+6+3 nitrogen atoms.

With respect to a rational planning of the synthesis of microporous nitridozeolites it may be important, that the anions $[\text{BN}_3]^{6-}$ are situated in the $[6^{14}]$ cages of the $[\text{Si}_{12}\text{X}_{24}]$ framework structure (Figure 2 and Figure 3). Conceivable though not yet proven is the assumption that initially during the formation of $\text{Ba}_4\text{Ln}_7[\text{Si}_{12}\text{N}_{23}\text{O}][\text{BN}_3]$ the $[\text{BN}_3]^{6-}$ ions were excised from the boron nitride layers. Subsequently these $[\text{BN}_3]^{6-}$ units do not condense with the nitridosilicate framework but presumably they act as high-temperature stable

templates around which the $[\text{Si}_{12}\text{N}_{23}\text{O}]$ framework is organized.

The structure determination with single-crystal X-ray diffraction data gave no evidence for the localization of oxygen. In general there are two possible models: The oxygen atoms may either be localized in the BX_3 units or in the $\text{Si}_{12}\text{X}_{24}$ network structure. To achieve a crystallographic differentiation of O and N, we performed both lattice energy calculations using the Ewald procedure (MAPLE, Madelung part of lattice energy)^[13] as well as bond-length bond-strength calculations and we also considered possible crystallographic supercells or lower space group symmetries. However no indications for a crystallographic ordering of O and N were obtained.

Theoretically, vibrational spectroscopy or solid-state NMR investigations should be suitable to distinguish between the possible anions $[\text{BN}_3]^{6-}$, $[\text{BN}_2\text{O}]^{5-}$, or $[\text{BNO}_2]^{4-}$. Due to the strong dipolar influence of the unpaired electrons of Nd fairly broad linewidths were observed in the recorded ^{11}B MAS NMR spectrum of $\text{Ba}_4\text{Nd}_7[\text{Si}_{12}\text{N}_{23}\text{O}][\text{BN}_3]$. On the basis of these data a reliable discrimination whether the quadrupolar coupling tensor was isotropic ($[\text{BN}_3]^{6-}$) or anisotropic ($[\text{BN}_2\text{O}]^{5-}$ or $[\text{BNO}_2]^{4-}$) was not possible. The FTIR spectra recorded from polycrystalline powder samples showed a superposition of the signals originating from the Si–X network and those of the BX_3 units. Due to the very strong absorption of the Nd compound (dark red color) single-crystal Raman spectra could not be obtained.

In summary we assume that the small extent of oxygen in $\text{Ba}_4\text{Ln}_7[\text{Si}_{12}\text{X}_{24}][\text{BX}_3]$ is randomly distributed between the X positions of the $[\text{Si}_{12}\text{X}_{24}]$ framework structure without crystallographic order, while the noncondensed trigonal-planar anions are exclusively $[\text{BN}_3]^{6-}$. In our opinion the occurrence of hitherto unknown $[\text{BN}_2\text{O}]^{5-}$ or $[\text{BNO}_2]^{4-}$ seems unlikely but not impossible. The occurrence of $[\text{BN}_3]^{6-}$ is further confirmed by the high-quality crystallographic determination of the bond lengths and angles in these anions in combination with small and reasonable anisotropic thermal displacement ellipsoids (Figure 1), which correspond well with the geometric data of $[\text{BN}_3]^{6-}$ ions in other nitridoborates (e.g. $\text{La}_5\text{B}_4\text{N}_9$, $\text{Ce}_{15}\text{B}_8\text{N}_{25}$) and with the B–N bond lengths of tris(amino), bis(amino)organo, or amino(di-organo)boranes without π interactions (145–148 pm).^[14–17] In contrast, typical B–O bond lengths are significantly smaller (e.g. 138.4 pm in $\text{Ca}_3[\text{BO}_3]_2$).^[18]

Conclusion

Isolated $[\text{BN}_3]^{6-}$ ions embedded in an oxonitridosilicate framework structure were observed in the series $\text{Ba}_4\text{Ln}_7[\text{Si}_{12}\text{N}_{23}\text{O}][\text{BN}_3]$ with $\text{Ln} = \text{Pr}, \text{Nd}, \text{Sm}$. From theoretical considerations concerning the formation mechanism of these compounds the assumption of a template-directed synthesis, during which the orthonitridoborate ions act as high-temperature stable templates seems likely. Apparently there is no tendency for the formation of condensed Si–B–N network structures of corner-sharing BN_3 and SiN_4 units in this system.

Experimental Section

Silicon diimide: In a three-necked bottle CH_2Cl_2 (50 mL, Merck, p. a.) was saturated with NH_3 (99.9%, BASF, dried by condensation on sodium and potassium) under a dried argon atmosphere. A precooled solution of SiCl_4 (20 mL, 0.17 mol, Merck) in CH_2Cl_2 (30 mL) was slowly added with stirring. Afterwards the suspension was carefully allowed to warm up to room temperature under a NH_3 atmosphere [Eq. (1)]. For purification from NH_4Cl the finely powdered residue was heated in a NH_3 gas flow to 300°C and finally to 600°C .^[19] The resulting product is a white X-ray amorphous powder with the approximate analytical composition $\text{Si}(\text{NH})_2$. It is relatively undefined but very reactive. Silicon diimide is an important precursor compound for the technical production of Si_3N_4 ceramics.^[19]



Poly(boron amide imide): The synthesis of poly(boron amide imide) was performed similarly to that of silicon diimide,^[5] however, BBr_3 was used instead of SiCl_4 . The purification from the by-product NH_4Br was achieved by heating the raw product to temperatures of 480°C and finally 600°C .

$\text{Ba}_4\text{Ln}_7[\text{Si}_{12}\text{N}_{23}\text{O}][\text{BN}_3]$ with $\text{Ln} = \text{Pr}, \text{Nd}, \text{Sm}$: In a characteristic reaction batch Ba (0.99 mmol; 99.9%, ABCR), Pr (1.00 mmol; 99.9%, ABCR), $\text{Si}(\text{NH})_2$ (1.67 mmol), BaCO_3 (0.10 mmol; 99%, Grössing/Filsum), and 37.9 mg poly(boron amide imide) were thoroughly mixed in a glove box under a purified argon atmosphere. Under nitrogen (1 bar, 5.0 Linde) the mixture then was transferred into a tungsten crucible positioned in the center of a quartz glass reactor of the radiofrequency furnace.^[4] Within 1 h the crucible was heated to 1000°C and then within 4 h to 1650°C . The reaction mixture was kept at this temperature for 4 h and finally it was cooled to 1200°C within 9 h and subsequently quenched to room temperature. Dark green crystals up to 2 mm of $\text{Ba}_4\text{Pr}_7[\text{Si}_{12}\text{N}_{23}\text{O}][\text{BN}_3]$ were obtained with a yield of approximately 70%. The crystals were embedded in a glass melt of very high mechanical hardness. The crystals had to be mechanically separated from this glass phase by the use of severe mechanical force. Usually *h*-BN was observed as a further by-product, and it was separated in an inert solvent (cyclohexane, 99.5%, Merck) by the application of ultrasound. The isotopic compounds $\text{Ba}_4\text{Sm}_7[\text{Si}_{12}\text{N}_{23}\text{O}][\text{BN}_3]$ and $\text{Ba}_4\text{Nd}_7[\text{Si}_{12}\text{N}_{23}\text{O}][\text{BN}_3]$ were synthesized in the same manner and they have been obtained as large orange-brown and dark red crystals, respectively.

Chemical analyses: In accordance with the X-ray structure analysis the analytical compositions of the three compounds $\text{Ba}_4\text{Ln}_7[\text{Si}_{12}\text{N}_{23}\text{O}][\text{BN}_3]$ with $\text{Ln} = \text{Pr}, \text{Nd}, \text{or Sm}$, were confirmed by energy-dispersive X-ray microanalysis (Ln, Ba, Si). Additionally, for the samarium compound a quantitative elemental analysis was performed by the analytical laboratory Pascher, Remagen/Germany. Elemental analysis calcd (%) for $\text{Ba}_4\text{Sm}_7\text{Si}_{12}\text{N}_{26}\text{O}$ (2339.84): Ba 23.6, Sm 45.2, Si 14.5, B 0.5, N 15.6, O 0.7; found: Ba 23.9, Sm 45.2, Si 14.1, B 0.5, N 15.7, O 0.8. The absence of hydrogen (NH) was proven by IR spectroscopy.

Magnetic measurements: The magnetic susceptibilities of polycrystalline samples of $\text{Ba}_4\text{Nd}_7[\text{Si}_{12}\text{N}_{23}\text{O}][\text{BN}_3]$ were measured with a MPMS XL SQUID magnetometer (Quantum Design) in the temperature range 4.2 to 300 K with magnetic flux densities up to 5 T. A sample of 10.586 mg was placed into a small gelatine capsule and fixed within a thin-walled polymer straw mounted at the sample holder rod. The sample was then cooled to 4.2 K in a zero magnetic field and slowly heated to room temperature in an applied external field.

The temperature dependence of the inverse magnetic susceptibility of $\text{Ba}_4\text{Nd}_7[\text{Si}_{12}\text{N}_{23}\text{O}][\text{BN}_3]$ is displayed in Figure 6. The compound shows Curie–Weiss behavior above 60 K with an experimental magnetic moment of $\mu_{\text{exp}} = 3.36(5) \mu_{\text{B}}/\text{Nd}$ atom. This is close to the value of $\mu_{\text{eff}} = 3.62 \mu_{\text{B}}$ for the free Nd^{3+} ion.^[20, 21] The paramagnetic Curie temperature (Weiss constant) of $\Theta = -22(1) \text{K}$ was obtained by linear extrapolation of the $1/\chi$ versus T data to $1/\chi = 0$. The deviation from Curie–Weiss behavior below about 60 K may be attributed to crystal field splitting of the $J = 9/2$ ground state of the Nd^{3+} ions.^[20, 21] No magnetic ordering is evident down to 4.2 K.

The magnetization isotherms at 4.2 and 290 K are displayed in Figure 7. As expected for a paramagnetic material, a linear increase of the magnetization is observed at 290 K. A field-induced increase of the magnetization is evident at 4.2 K. At the highest obtainable field strength of 5 T the magnetization was $1.11(1) \mu_{\text{B}}/\text{Nd}$, which is significantly smaller than the calculated value of $3.27 \mu_{\text{B}}/\text{Nd}$ according to $g \times J$.^[21]

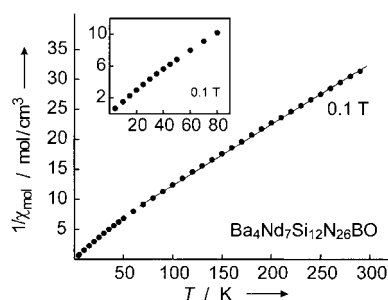


Figure 6. Temperature dependence of the reciprocal magnetic susceptibility of $\text{Ba}_4\text{Nd}_7\text{Si}_{12}\text{N}_{26}\text{BO}$ measured at an external magnetic flux density of 0.1 T. The solid line indicates the range for the Curie–Weiss fit. The low-temperature data are shown in the inset.

Crystal structure analysis: X-ray diffraction data were collected on a four-circle diffractometer (Siemens P4). The space group was determined to be $P\bar{6}$ (no. 174) in accord with the absence of any extinction conditions for the hexagonal lattice. The unit cell and the space group were verified by a simulation of Buerger exposures of the X-ray data from an IPDS-measurement in combination with a search of possible supercell reflections.^[22] Additionally, all reflections detected by X-ray powder diffractometry (Siemens D5000) of single-phase $\text{Ba}_4\text{Ln}_7[\text{Si}_{12}\text{N}_{23}\text{O}][\text{BN}_3]$ with Ln = Pr, Nd, Sm have been indexed and their observed intensities agree well with the calculated diffraction patterns based on the single-crystal data. The lattice parameters decrease from the praseodymium to the samarium

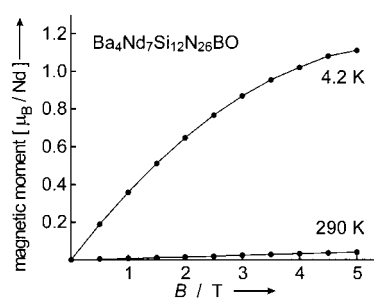


Figure 7. Magnetization isotherms of $\text{Ba}_4\text{Nd}_7\text{Si}_{12}\text{N}_{26}\text{BO}$ at 4.2 and 290 K.

compound as expected from the lanthanoid contraction. The crystal structure of $\text{Ba}_4\text{Pr}_7[\text{Si}_{12}\text{N}_{23}\text{O}][\text{BN}_3]$ was solved by direct methods using Xstep32^[23] and refined with anisotropic displacement parameters for all atoms. As a check for the correct site assignment (the scattering power of barium and praseodymium is very similar), the occupancy parameters of these atoms were refined in a separate series of least-squares cycles along with the displacement parameters. These refinements clearly revealed three praseodymium and two barium positions in good agreement with the magnetic data discussed above. The Rietveld refinement has been performed with the program GSAS^[24] using the X-ray single-crystal data of $\text{Ba}_4\text{Pr}_7[\text{Si}_{12}\text{N}_{23}\text{O}][\text{BN}_3]$ as a starting model.

Relevant crystallographic data and details of the X-ray data collection are shown in Table 1. Table 2 gives the positional and displacement parameters

Table 1. Crystallographic data for $\text{Ba}_4\text{Ln}_7[\text{Si}_{12}\text{N}_{23}\text{O}][\text{BN}_3]$ with Ln = Pr, Nd, and Sm.

	$\text{Ba}_4\text{Pr}_7[\text{Si}_{12}\text{N}_{23}\text{O}][\text{BN}_3]$	$\text{Ba}_4\text{Nd}_7[\text{Si}_{12}\text{N}_{23}\text{O}][\text{BN}_3]$	$\text{Ba}_4\text{Sm}_7[\text{Si}_{12}\text{N}_{23}\text{O}][\text{BN}_3]$
formula weight [g mol^{-1}]	2263.67	2287.00	2329.84
crystal system, space group		hexagonal, $P\bar{6}$ (no. 174)	
X-ray powder diffraction radiation	Siemens D 5000	STOE Stadi P $\text{Mo}_{\text{K}\alpha 1}$ ($\lambda = 70.93$ pm)	STOE Stadi P germanium monochromator
unit cell dimensions [pm] (Rietveld refinement)	quartz monochromator $a = 1227.33(2)$ $c = 545.74(2)$	$a = 1224.32(1)$ $c = 545.135(7)$	$a = 1220.76(2)$ $c = 544.50(1)$
X-ray four-circle diffractometer radiation		Siemens P4 $\text{Mo}_{\text{K}\alpha}$ ($\lambda = 71.073$ pm, graphite monochromator)	
unit cell dimensions [pm]	$a = 1225.7(1)$ $c = 544.83(9)$	$a = 1222.6(1)$ $c = 544.6(1)$	$a = 1215.97(5)$ $c = 542.80(5)$
cell volume [10^6 pm ³]	708.8(2)	704.9(2)	695.05(8)
Z		1	
X-ray density [g cm^{-3}]	5.299	5.383	5.562
$F(000)$	999	1006	1020
absorption coefficient [mm^{-1}]	17.798	18.691	20.668
temperature [K]	292(2)	293(2)	293(2)
crystal size [mm ³]	$0.10 \times 0.12 \times 0.15$	$0.10 \times 0.20 \times 0.22$	$0.06 \times 0.06 \times 0.48$
diffraction range [$^\circ$]	$4^\circ \leq 2\theta \leq 55^\circ$	$4^\circ \leq 2\theta \leq 60^\circ$	$4^\circ \leq 2\theta \leq 95^\circ$
h, k, l	$-15 \leq h \leq 15$ $-13 \leq k \leq 13$ $-7 \leq l \leq 7$; octants: 2	$-16 \leq h \leq 16$ $-17 \leq k \leq 17$ $-7 \leq l \leq 7$; octants: 2	$-1 \leq h \leq 25$ $-23 \leq k \leq 1$ $-11 \leq l \leq 1$; octants: 2
scan type, speed	$\omega, 2^\circ \text{ min}^{-1}$	$\omega, 2^\circ \text{ min}^{-1}$	$\omega, 2^\circ \text{ min}^{-1}$
total no. reflections	6328	3048	5634
independent reflections	1211 ($R_{\text{int}} = 0.0245$)	1505 ($R_{\text{int}} = 0.0275$)	4427 ($R_{\text{int}} = 0.0287$)
observed reflections ($I > 2\sigma I$)	1207	1499	4098
refined parameters	98	92	98
I/σ	39.19	47.56	24.33
corrections		Lorentz, polarization, absorption habitus ^[26]	
absorption correction			
min./max. transmission	0.1514/0.3440	0.1746/0.3182	0.1869/0.2391
Flack parameter	0.01(3)	0.00(2)	-0.01(2)
extinction coefficient	0.0102(2)	0.0054(2)	0.0184(7)
min./max. residual electron density [$e/\text{\AA}^3$]	-0.807/1.972	-0.977/1.440	-4.729/3.215
GOF	1.123	1.097	1.051
R indices (all data)	$R1 = 0.0127$ $wR2 = 0.0304$	$R1 = 0.0169$ $wR2 = 0.0393$	$R1 = 0.0467$ $wR2 = 0.0988$

Table 2. Atomic coordinates and anisotropic displacement parameters [pm^2] for $\text{Ba}_4\text{Pr}_7[\text{Si}_{12}\text{N}_{23}\text{O}][\text{BN}_3]$ determined by single-crystal X-ray diffraction with esds in parentheses. U_{eq} is defined as one third of the trace of the orthogonalized U_{ij} tensor. The anisotropic displacement factor exponent is of the form $-2\pi^2[(ha^*)^2U_{11} + \dots + hka^*b^*U_{12}]$.

Atom	Wyckoff position	x	y	z	U_{11}	U_{22}	U_{33}	U_{23}	U_{13}	U_{12}	U_{eq}
Ba(1)	3k	0.56991(4)	0.08287(4)	1/2	153(2)	167(2)	122(2)	0	0	109(2)	135(1)
Ba(2)	1d	1/3	2/3	1/2	215(2)	215(2)	69(3)	0	0	107(2)	166(2)
Pr(1)	3j	0.03693(3)	0.32628(3)	0	52(2)	58(2)	131(2)	0	0	21(2)	84(1)
Pr(2)	3j	0.25298(4)	0.22269(4)	0	111(2)	84(2)	55(2)	0	0	70(2)	73(1)
Pr(3)	1b	0	0	1/2	106(2)	106(2)	134(3)	0	0	53(1)	115(2)
Si(1)	3k	0.1992(2)	0.3230(2)	1/2	51(8)	61(7)	55(7)	0	0	33(7)	53(3)
Si(2)	3k	0.3121(2)	0.1188(2)	1/2	44(7)	48(8)	41(7)	0	0	22(7)	45(3)
Si(3)	3j	0.3076(2)	0.5075(2)	0	39(7)	50(8)	48(7)	0	0	30(6)	43(3)
Si(4)	3j	0.5063(2)	0.2337(2)	0	48(7)	47(8)	47(7)	0	0	14(6)	52(3)
B	1a	0	0	0	40(30)	40(30)	50(50)	0	0	20(20)	40(20)
N/O(1)	6l	0.2773(4)	0.4067(3)	0.2437(7)	120(20)	80(20)	60(20)	2(2)	3(2)	50(10)	83(7)
N/O(2)	6l	0.4029(4)	0.1685(4)	0.2419(7)	70(20)	130(20)	60(20)	0(2)	2(2)	30(20)	97(7)
N/O(3)	3k	0.0434(7)	0.2820(6)	1/2	60(30)	140(30)	250(30)	0	0	60(20)	150(20)
N/O(4)	3k	0.2143(5)	0.1849(5)	1/2	120(30)	40(20)	80(20)	0	0	50(20)	70(10)
N(5)	3j	0.0183(7)	0.1281(6)	0	210(30)	80(30)	220(30)	0	0	100(20)	160(20)
N/O(6)	3j	0.1887(6)	0.5489(6)	0	70(30)	50(30)	250(30)	0	0	30(20)	120(20)
N/O(7)	3j	0.6086(6)	0.1775(6)	0	110(30)	140(30)	80(30)	0	0	90(20)	100(20)

for all atoms. Table 3 and 4 contain selected interatomic distances and angles.^[25] The Rietveld refinement of the X-ray diffraction data is illustrated in Figure 8, the results of the final refinement are summarized in Table 5.

Thermogravimetric investigations: For the measurements a sample of $\text{Ba}_4\text{Sm}_7[\text{Si}_{12}\text{N}_{23}\text{O}][\text{BN}_3]$ (22.475 mg) was placed in a small tungsten crucible. The investigations were performed in a DTA-TG thermoanalytical balance TGA 92–2400, Setaram, Caluire/France with a measurement rod 92–2400-TG-ATG 2400 °C made of tungsten. The sample was heated under an atmosphere of helium at 25 K min^{-1} to 500 °C followed by a slower increase of temperature (10 K min^{-1}) up to 1600 °C. The result is shown in Figure 9. Similar to other nitridosilicates obtained in our group $\text{Ba}_4\text{Sm}_7[\text{Si}_{12}\text{N}_{23}\text{O}][\text{BN}_3]$ exhibits a thermal stability up to 1400 °C and it is resistant against hydrolysis. At higher temperatures a rapid decomposition and the formation of gaseous products and an X-ray amorphous solid residue is observed.

Solid-state NMR investigation: Despite the paramagnetic character of $\text{Ba}_4\text{Nd}_7[\text{Si}_{12}\text{N}_{23}\text{O}][\text{BN}_3]$ a ^{11}B -MAS NMR spectrum could be recorded.

Owing to the strong dipolar influence of the unpaired electrons of Nd the interpretation of the NMR spectrum is difficult.

Table 4. Interatomic angles [$^\circ$] in the structure of $\text{Ba}_4\text{Pr}_7[\text{Si}_{12}\text{N}_{23}\text{O}][\text{BN}_3]$ determined by single-crystal X-ray diffraction with esds in parentheses.

N/O(1)-Si(1)-N/O(4)	106.0(2) ($2 \times$)	N/O(1)-Si(3)-N/O(1)	100.8(3)
N/O(1)-Si(1)-N/O(1)	109.1(3)	N/O(1)-Si(3)-N/O(6)	107.0(2) ($2 \times$)
N/O(3)-Si(1)-N/O(4)	110.5(3)	N/O(6)-Si(3)-N/O(6)	109.6(4)
N/O(1)-Si(1)-N/O(3)	112.5(2) ($2 \times$)	N/O(1)-Si(3)-N/O(6)	115.8(2) ($2 \times$)
N/O(2)-Si(2)-N/O(3)	106.4(2) ($2 \times$)	N/O(2)-Si(4)-N/O(2)	99.8(3)
N/O(2)-Si(2)-N/O(4)	108.1(2) ($2 \times$)	N/O(2)-Si(4)-N/O(7)	109.4(2) ($2 \times$)
N/O(2)-Si(2)-N/O(2)	111.1(3)	N/O(2)-Si(4)-N/O(7)	109.8(2) ($2 \times$)
N/O(3)-Si(2)-N/O(4)	116.7(3)	N/O(7)-Si(4)-N/O(7)	117.3(4)
Si(1)-N/O(1)-Si(3)	155.9(3)	Si(2)-N/O(2)-Si(4)	173.5(3)
Si(1)-N/O(3)-Si(2)	161.6(4)	Si(2)-N/O(4)-Si(1)	148.8(4)
Si(3)-N/O(6)-Si(3)	130.4(4)	Si(4)-N/O(7)-Si(4)	122.7(4)

Table 3. Interatomic distances [pm] in the structure of $\text{Ba}_4\text{Pr}_7[\text{Si}_{12}\text{N}_{23}\text{O}][\text{BN}_3]$ determined by single-crystal X-ray diffraction with esds in parentheses.

Ba(1)–N/O(7)	290.5(2)	($2 \times$)	Pr(3)–N/O(4)	246.6(5)	($3 \times$)
Ba(1)–N/O(2)	306.8(4)	($2 \times$)	Pr(3)–N(5)	309.6(3)	($6 \times$)
Ba(1)–N/O(1)	309.0(4)	($2 \times$)	Pr(3)–N/O(3)	322.4(7)	($3 \times$)
Ba(1)–N/O(2)	312.3(4)	($2 \times$)	B–N(5)	147.1(6)	($3 \times$)
Ba(1)–N/O(4)	338.1(6)		Si(1)–N/O(1)	171.4(4)	($2 \times$)
Ba(1)–N/O(3)	354.9(7)		Si(1)–N/O(3)	171.5(7)	
Ba(2)–N/O(6)	317.6(3)	($6 \times$)	Si(1)–N/O(4)	179.2(5)	
Ba(2)–N/O(1)	322.3(4)	($6 \times$)	Si(2)–N/O(2)	170.6(4)	($2 \times$)
Pr(1)–N(5)	232.3(6)		Si(2)–N/O(3)	172.4(7)	
Pr(1)–N/O(6)	241.5(6)		Si(2)–N/O(4)	175.1(6)	
Pr(1)–N/O(2)	255.2(4)	($2 \times$)	Si(3)–N/O(6)	169.5(7)	
Pr(1)–N/O(3)	278.6(2)	($2 \times$)	Si(3)–N/O(1)	172.3(4)	($2 \times$)
Pr(1)–N/O(1)	291.7(4)	($2 \times$)	Si(3)–N/O(6)	176.6(6)	
Pr(2)–N/O(1)	250.3(4)	($2 \times$)	Si(4)–N/O(7)	168.6(7)	
Pr(2)–N(5)	250.7(7)		Si(4)–N/O(7)	170.6(7)	
Pr(2)–N(5)	257.3(7)		Si(4)–N/O(2)	172.3(4)	($2 \times$)
Pr(2)–N/O(2)	260.3(4)	($2 \times$)			
Pr(2)–N/O(4)	276.4(1)	($2 \times$)			

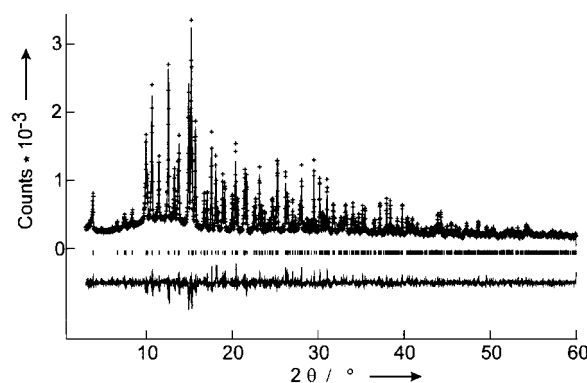
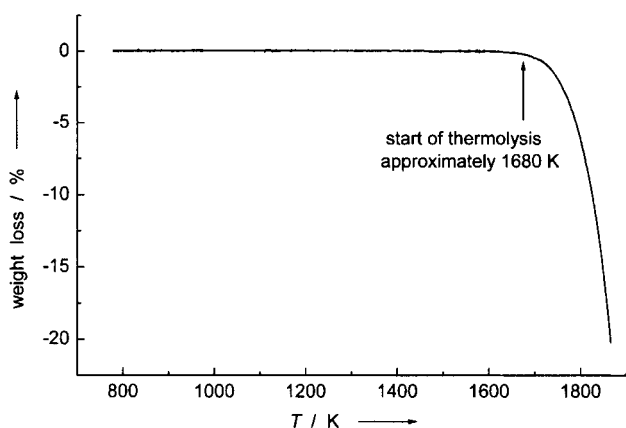


Figure 8. X-ray powder diffraction pattern and difference profile of the Rietveld refinement of $\text{Ba}_4\text{Pr}_7[\text{Si}_{12}\text{N}_{23}\text{O}][\text{BN}_3]$. Allowed peak positions are marked by vertical lines; crosses and lines indicate observed and calculated results, respectively. The diffraction pattern was recorded on a D5000 diffractometer (Siemens) using $\text{MoK}\alpha$ radiation (70.93 pm).

Table 5. Results of the Rietveld refinements for Ba₄Pr₇[Si₁₂N₂₃O][BN₃] and Ba₄Nd₇[Si₁₂N₂₃O][BN₃].

	Ln = Pr	Ln = Nd
crystal system	hexagonal	
space group	<i>P</i> 6̄ (no. 174)	
diffractometer	Siemens D5000	STOE Stadi P
λ [pm]	70.93 (MoK _α)	
T [K]	293(2)	293(2)
lattice parameters [pm]	<i>a</i> = 1227.33(2) <i>c</i> = 545.74(1)	<i>a</i> = 1224.32(1) <i>c</i> = 545.135(7)
cell volume [10 ⁶ pm ³]	711.94(2)	707.66(2)
Z	1	1
range [2θ]	3–60°	3–60°
no. of data points	5700	5700
refined parameters	40 (structure) 15 (profile)	35 (structure) 14 (profile)
R _p	0.0662	0.0580
wR _p	0.0880	0.0732
R	0.0671	0.0564
R(F ²)	0.1132	0.0965
χ ²	1.827	0.8323

Figure 9. Thermogravimetric measurement of Ba₄Sm₇[Si₁₂N₂₃O][BN₃]. Sample size 22.475 mg, heating rate 10 K min⁻¹, He atmosphere.

Acknowledgements

Generous financial support by the Fonds der Chemischen Industrie, Germany, and especially the Deutsche Forschungsgemeinschaft (Schwerpunktprogramm "Nitridobrücken", project SCHN 377/7 and Gottfried Wilhelm Leibniz grant) is gratefully acknowledged. The authors would like to thank Dr. Jürgen Senker, Department of Chemistry, University of Munich (LMU) for the solid-state NMR investigations, and Prof. Dr. H.-D. Lutz, University of Siegen, for the Raman measurements.

- [1] W. Schnick, *Angew. Chem.* **1993**, *105*, 846; *Angew. Chem. Int. Ed. Engl.* **1993**, *32*, 806.
- [2] H.-P. Baldus, M. Jansen, *Angew. Chem.* **1997**, *109*, 338; *Angew. Chem. Int. Ed. Engl.* **1997**, *36*, 255.
- [3] a) J. C. Schön, M. Jansen, *Angew. Chem.* **1996**, *108*, 1359; *Angew. Chem. Int. Ed. Engl.* **1996**, *35*, 1285; b) P. Kroll, R. Hofmann, *Angew. Chem.* **1998**, *110*, 2616; *Angew. Chem. Int. Ed. Engl.* **1998**, *37*, 2527.
- [4] W. Schnick, H. Huppertz, R. Lauterbach, *J. Mater. Chem.* **1999**, *9*, 289.
- [5] M. Orth, W. Schnick, *Z. Anorg. Allg. Chem.* **1999**, *625*, 551.
- [6] H. Hillebrecht, J. Curda, L. Schröder, H. G. von Schnering, *Z. Kristallogr.* **1993**, *Suppl.* *7*, 80.
- [7] J. Gaude, P. L'Haridon, J. Guyader, J. Lang, *J. Solid State Chem.* **1985**, *59*, 143.
- [8] O. Reckweg, H.-J. Meyer, *Z. Anorg. Allg. Chem.* **1999**, *625*, 866.
- [9] a) W. E. Klee, *Z. Kristallogr.* **1987**, *179*, 67; b) A. Beukemann, W. E. Klee, *Z. Kristallogr.* **1994**, *209*, 709.
- [10] W. M. Meier, D. H. Olson, *Atlas of Zeolite Structure Types*, Butterworths, London **1987**.
- [11] W. H. Baur, *Crystallogr. Rev.* **1987**, *1*, 59.
- [12] R. D. Shannon, C. T. Prewitt, *Acta Crystallogr. Sect. B* **1969**, *25*, 925.
- [13] a) R. Hoppe, *Angew. Chem.* **1966**, *78*, 52; *Angew. Chem. Int. Ed. Engl.* **1966**, *5*, 95; b) R. Hoppe, *Angew. Chem.* **1970**, *82*, 7; *Angew. Chem. Int. Ed. Engl.* **1970**, *9*, 25.
- [14] G. Bullen, N. H. Clark, *J. Chem. Soc. Chem. Commun.* **1967**, 670.
- [15] R. A. Bartlett, X. Feng, M. M. Olmstead, P. P. Power, K. J. Weese, *J. Am. Chem. Soc.* **1987**, *109*, 4851.
- [16] M. Hildenbrand, H. Pritzkow, U. Zenneck, W. Siebert, *Angew. Chem.* **1984**, *96*, 371; *Angew. Chem. Int. Ed. Engl.* **1984**, *23*, 371.
- [17] S. Y. Shaw, D. A. Du Bois, W. H. Watson, R. H. Neilson, *Inorg. Chem.* **1988**, *27*, 974.
- [18] A. Vegas, F. H. Cano, S. Garcia-Blanco, *Acta Crystallogr. Sect. B* **1982**, *24*, 1968.
- [19] H. Lange, G. Wötting, G. Winter, *Angew. Chem.* **1991**, *103*, 1606; *Angew. Chem. Int. Ed. Engl.* **1991**, *211*, 254.
- [20] A. Szytuła, J. Leciejewicz, *Handbook of Crystal Structures and Magnetic Properties of Rare Earth Intermetallics*, CRC Press, Boca Raton, Florida, **1994**.
- [21] H. Lueken, *Magnetochemie*, Teubner, Stuttgart, **1999**.
- [22] SPACE, Revision 2.87, **1997**, STOE & Cie GmbH, Darmstadt.
- [23] Xstep32, Revision 1.05b, **1999**, STOE & Cie GmbH, Darmstadt.
- [24] R. B. von Dreele, A. C. Larson, General Structure Analysis System, Los Alamos National Laboratory Report LAUR 86–748, **1990**.
- [25] Further details on the crystal structure investigations may be obtained from the Fachinformationszentrum Karlsruhe, D-76344 Eggenstein-Leopoldshafen, (Germany, fax: + (49) 7247-808-666; e-mail: crysdata@fiz-karlsruhe.de), on quoting the depository numbers CSD-411450 (Ba₄Sm₇[Si₁₂N₂₃O][BN₃]), CSD-411451 (Ba₄Pr₇[Si₁₂N₂₃O][BN₃]), and CSD-411452 (Ba₄Nd₇[Si₁₂N₂₃O][BN₃]).
- [26] XRED, Revision 1.19, **1999**, STOE & Cie GmbH, Darmstadt.

Received: January 25, 2001 [F 3023]